Available online at www.sciencedirect.com

ScienceDirect

Ceramics International 40 (2014) 4909–4915

CERAMICS INTERNATIONAL

www.elsevier.com/locate/ceramint

Apatite formation on alumina: The role of the initial adsorption of calcium and phosphate ions

Juan Coreño-Alonso[a,*], Oscar Coreño-Alonso[b], J. Merced Martínez-Rosales[c]

[a]*Area Académica de Ciencias de la Tierra y Materiales, Universidad Autónoma del Edo, de Hidalgo, Carretera Pachuca-Tulancingo, km 4.5, Mineral de la Reforma, Hgo, Mexico*
[b]*Departamento de Ingeniería Civil, Universidad de Guanajuato, Avenida Juárez 77, Centro, Guanajuato, Gto, Mexico*
[c]*Departamento de Química, Universidad de Guanajuato, Colonia Noria Alta s/n, Guanajuato, Gto, Mexico*

Received 1 August 2013; received in revised form 9 October 2013; accepted 16 October 2013
Available online 25 October 2013

Abstract

Apatite formation on alumina was studied using two different pretreatments: the previous adsorption of calcium or phosphate ions before its immersion on two calcium-phosphate solutions. At pH 7.4, alumina that adsorbed initially phosphate and then calcium ions was used as substrate, but no apatite growth was detected after 16 days of immersion. However, apatite growth was observed at pH 8.6. In this case, alumina was first immersed in a calcium solution at pH 11.3, later suspended in a phosphate solution, and finally in a calcium-phosphate solution at pH 8.6. Results indicate that, when phosphate ions are firstly attached to the alumina surface at pH 7.4, although they attract calcium ions, apatite nucleation is inhibited. On the contrary, it seems that the initial calcium adsorption to the alumina surface forms appropriate sites for apatite nucleation and growth. Apparently, the alumina positive surface charge is not directly responsible for its inability towards apatite nucleation at pH 7.4, as has been previously suggested.

Keywords: B. Surfaces; C. Apatite; C. Alumina; E. Biomedical applications

1. Introduction

Chemical coatings of calcium phosphate apatite on different substrates have been reported for more than 20 years. The aim of these studies is to search for better techniques to coat mainly metallic surfaces; however, organic polymers and ceramics have also been investigated [1,2]. A number of works have been devoted to understand which characteristics a surface must fulfill to be a good substrate for apatite growth. The most widely studied surfaces have been sol–gel silica, bioglasses [3–8], sol–gel TiO_2, Ti and its alloys [9–13] due to their well known ability as apatite growth promoters. Besides, some other surfaces like calcium titanate [14], tantalum metal [15], zirconia gel [16], functionalized organic monolayers formed on several surfaces [17–19] and alumina [9,20–23] have also been studied.

With regard to surface chemical characteristics, it has been suggested that Si-OH [4,7,22], Ti-OH[12,22], Ta-OH [15] and Zr-OH [16] groups are effective apatite nucleation centers. Besides, functional groups other than OH, such as $–PO_4H$ and –COOH have also shown capacity to form apatite on some substrates [17–19].

Concerning the physical characteristics associated with apatite nucleation, one of the most commonly observed and accepted is the development of a negative surface charge at pH 7.4 when the substrate is immersed in an electrolyte aqueous solution. It is generally proposed that a negative surface attracts calcium ions, being the calcium attachment the first step on the apatite nucleation. Afterwards, phosphate ions are attracted [1,3,9,10,22,23], which would explain the zeta potential variations measured during the apatite formation [1,9,24]. Alumina inertness towards apatite growth has been

---

*Corresponding author. Tel.: +52 771 717 2000x2281.
E-mail addresses: jcoreno@uaeh.edu.mx, jcorenoalonso@gmail.com (J. Coreño-Alonso), ocoreno@yahoo.com (O. Coreño-Alonso), mercedj@ugto.mx (J. Merced Martínez-Rosales).

0272-8842/$ - see front matter © 2013 Elsevier Ltd and Techna Group S.r.l. All rights reserved.
http://dx.doi.org/10.1016/j.ceramint.2013.10.079

explained arguing its positive surface charge at pH 7.4 [9,10,22,23] and a lack of affinity of Al-OH groups for calcium and phosphate ions [21]. The aim of this paper is to study the capacity of alumina, which has initially adsorbed calcium or phosphate ions, to growth apatite using calcium-phosphate solutions at pH 7.4 and 8.6, trying to explain the possible effect of these ions and of the alumina surface charge on its apatite forming abilities.

2. Materials and methods

2.1. Calcium and phosphate adsorption

Starting from precursor pseudoboehmite, synthesized according to a previous work [25], Al_2O_3 (-325 mesh) powder was obtained by a thermal treatment of the precursor at 600 °C for 2 h.

Prior to use, alumina was washed with 10 mM NaOH (1 g, Al_2O_3/10 mL, NaOH). After stirring for 1 h, the suspension was centrifuged, and the solid was washed with deionized water to a constant conductivity of the supernatant. Finally, the solid was filtered, dried for 2 h at 110 °C, and ground using an agate mortar and pestle.

For each one of the adsorption experiments, 0.1 g of alumina was immersed for 1 week in 5 mL of deionized water at room temperature. Before using the alumina, the suspension was centrifuged to separate the water from the powder. Hereafter, the alumina obtained after an initial immersion in a phosphate or in a calcium solution is referred as Al_2O_3–PO_4 or Al_2O_3–Ca, respectively.

A set of experiments was performed to determine calcium adsorption once phosphate had been uptaken and vice versa. 0.1 g of the pristine alumina was immersed on 40 mL of a 1 mM Na_2HPO_4 and 0.14 M NaCl solution using deionized water at the desired pH. The resulting suspension was stirred at room temperature for 24 h. Then, it was centrifuged and the solid obtained, Al_2O_3–PO_4, was immersed in 10 mL of a 1 mM $CaCl_2$ and 0.14 M NaCl solution using deionized water at the same pH of the previous suspension. These experiments were performed at pH 7.4, 8.0 and 8.6. Each experiment was repeated three times. For all of the experiments, pH was adjusted with tris(hydroxymethyl aminomethane) and 0.1 M HCl except as noted.

On the other hand, 0.1 g of the alumina was immersed in 10 mL of a 1 mM $CaCl_2$ and 0.14 M NaCl solution using deionized water at the desired pH. The resulting suspension was stirred at room temperature for 24 h. Then, the suspension was centrifuged and the solid obtained, Al_2O_3–Ca, was immersed in 40 mL of a 1 mM Na_2HPO_4 and 0.14 M NaCl solution using deionized water at the same pH of the previous suspension.

After each 24 h immersion period, calcium or phosphate were measured. Calcium concentration was measured by titration with ethylenediaminotetraacetic acid disodium salt (EDTA), using eriochrome T black indicator. The phosphate concentration was measured by conventional molybdenum blue method.

2.2. Zeta (ζ) potential measurements and determination of the isoelectric point (IEP)

A stock suspension of alumina was prepared by adding 1 g of this powder to 100 mL of deionized water. The suspension was aged for at least 4 weeks and ultrasonically dispersed for 10 min prior to the ζ potential experiments. Measurements were carried out with 5 mL of the dispersed stock suspension, followed by addition of water and the necessary quantity of the respective salt to obtain the desired concentration of $CaCl_2$ or Na_2HPO_4. Finally, pH was adjusted with diluted HCl or NaOH solutions and each suspension was completed to 50 mL with deionized water. For all of the measurements, NaCl was used as background electrolyte. A potentiometer (Orion 720A) equipped with a combined electrode and automatic temperature compensation (ATC) probe was used to monitor the pH. The potentiometer was calibrated before each test with buffer solutions pH 4, 7 and 10. Before performing the ζ potential measurements, the suspensions were conditioned for at least 15 min.

2.3. Apatite growth tests on calcium-phosphate solutions at pH 7.4 and 8.6

We used two calcium-phosphate solutions, which contain only water, sodium, calcium, chloride, phosphate ions and the buffer.

pH 7.4.- Alumina (0.25 g) was immersed in 45 mL of a solution containing 0.14 M NaCl and 2 mM Na_2HPO_4 in deionized water at pH 7.4. The suspension was stirred for 24 h at room temperature. The solid obtained, Al_2O_3–PO_4, was centrifuged and suspended at pH 7.4 in 25 mL of a solution containing 0.14 M NaCl and 1 mM $CaCl_2$. After a 24 h period of mild stirring at room temperature, the solid, hereafter Al_2O_3–PO_4–Ca, was centrifuged and suspended in 30 mL of a solution containing 0.14 M NaCl, 2.5 mM $CaCl_2$ and 1 mM Na_2HPO_4 in deionized water at pH 7.4 at 37 °C. This calcium-phosphate solution has been employed previously for apatite growth on silica, titania and calcium titanate [14].

The suspension was mildly stirred for 24 h. Then, it was centrifuged, and the solid suspended again in 25 mL of the calcium-phosphate solution and stirred for 24 h at 37 °C. The solid was suspended two more times in 15 mL of calcium-phosphate solution at room temperature and stirred for 1 week period each time.

pH 8.6.- Alumina (0.05 g) was immersed in 5 mL of deionized water for at least 2 weeks. The suspension was centrifuged, and the solid was added to 5 mL of a 2 mM $CaCl_2$ solution. The initial pH of this solution was approximately 11.3, adjusted with NaOH. After 15 h of suspension at room temperature, the solid was centrifuged and washed with tris buffer solution at pH 8.6. Later, the solid, Al_2O_3–Ca, was suspended in 10 mL of a 0.15 M NaCl and 1 mM Na_2HPO_4 suspension at pH 8.6. After stirring for 5 h at room temperature, the solid was centrifuged and immersed 6 times at 30 °C in a calcium-phosphate solution at pH 8.6, under mild stirring, for 3 h lapses. Later, the solid was suspended overnight in

10 mL of a 1 mM $CaCl_2$ aqueous solution. After each suspension, the solid was washed once with 10 mL of deionized water. The above procedure was repeated twice. Finally, the solid was washed three times using deionized water.

The calcium-phosphate solution at pH 8.6 was prepared according to the following procedure. First, a phosphate solution was prepared by dissolving 0.005 mol of tris(hydroxymethyl aminomethane), 0.015 mol of NaCl and 10 mL of a 10 mM Na_2HPO_4 solution in 50 mL of deionized water. pH was adjusted to 8.6 by the addition of HCl 0.1 M, and deionized water was added to a final volume of 70 mL. Then, a calcium solution was prepared by diluting 4 mL of a 25 mM $CaCl_2$ solution in 30 mL of deionized water. Finally, the calcium solution was added dropwise to the vigorously stirred phosphate solution, at 30 °C.

2.4. Characterization techniques

The X-ray diffraction (XRD) pattern was obtained in an INEL diffractometer model Equinox 2000 using Cu Kα_1 radiation. ζ potential measurements were carried out with a Malvern Instruments Zetasizer 3000HSA. FTIR-Raman spectra were obtained using a Perkin-Elmer Spectrum GX FT-Raman spectrometer. The ^{31}P magic angle spinning (MAS) NMR spectra were obtained in a Varian Unity Plus 3000 MHz spectrometer with a 7 mm CP-MAS probe at 5 kHz. H_3PO_4 was used as reference. Surface area was determined with a Micromeritics Autosorb Automated ASAP 2010. Transmission electron microscopy (TEM) was performed in a Zeiss microscope Leo EM 910 at 120 kV.

3. Results and discussion

Fig. 1 shows the XRD pattern of the alumina powder used. All of the observed peaks correspond to a γ-Al_2O_3 according to the JPDF file 10-0425. The broadening of the peaks is associated with nanocrystalline structures of the sample and to a fraction of amorphous alumina. Fig. 2 corresponds to a bright field TEM image and a selected area electron diffraction pattern of the alumina obtained. In Fig. 2(a), a particle of around 200 nm can be observed, and in Fig. 2(b) the pattern shows a strong amorphous halo corresponding to the amorphous fraction of the alumina.

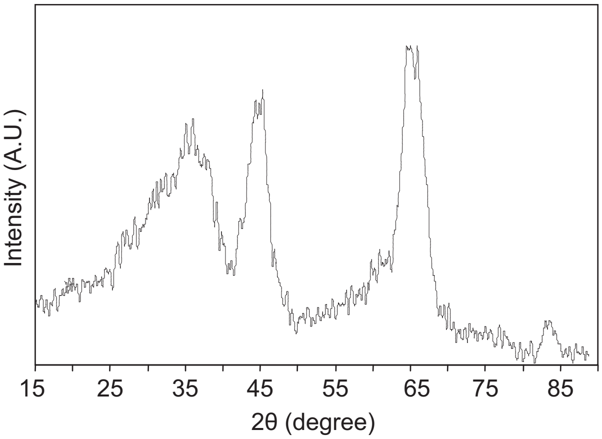

Fig. 1. XRD pattern of the alumina prepared by the hydrolysis precipitation method and dried for 2 h at 600 °C.

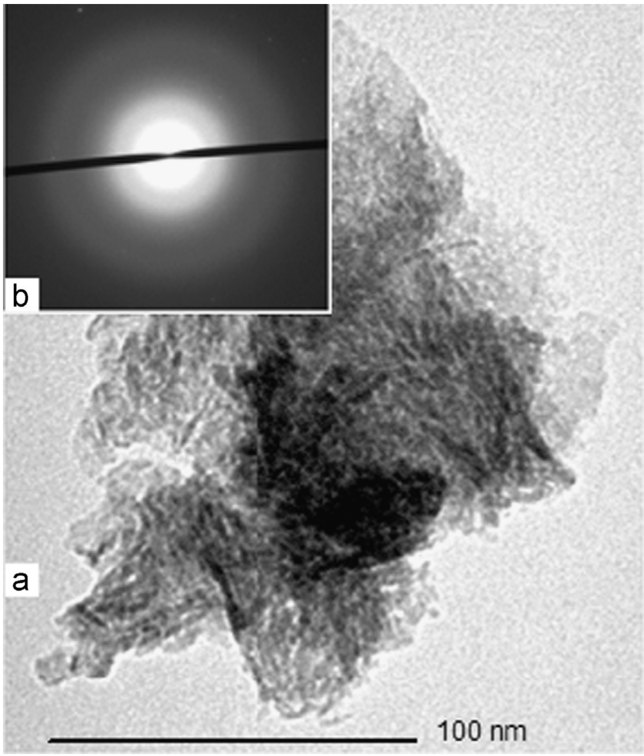

Fig. 2. TEM photograph (a) and selected area electron diffraction pattern (b) of the alumina prepared by the hydrolysis precipitation method and dried for 2 h at 600 °C.

The heat treatment of the pesudoboehmite precursor at 600 °C makes it possible to obtain a very high surface area, 313 m^2/g (BET method), which forms easily a hydrated surface layer when immersed in an aqueous solution. A high surface covered with plenty of Al-OH groups increases the chemisorption of calcium ions, and the possibility of formation of calcium phosphate nuclei for apatite growth becomes larger.

The alumina surface is positive up to pH 9, as can be seen in Fig. 3. It shows zeta (ζ) potential as a function of pH for three NaCl concentrations. The measured isoelectric point (IEP) was close to pH 9. This IEP is within the range reported for γ-Al_2O_3 [26]. NaCl is an indifferent electrolyte in this system because the determined IEP is independent of its ionic strength.

Fig. 4 shows the variation in ζ potential, as a function of pH, for alumina suspensions in the presence of calcium and phosphate ions and NaCl as background electrolyte. In the case of calcium ions (Fig. 4(b)), the IEP is shifted to a higher pH, around 10.5. This displacement is attributed to the specific adsorption of Ca ions on alumina according to the following equation [27,28]:

$$\equiv AlOH + Ca^{2+} \rightarrow \equiv AlOCa^{+} + H^{+} \quad (1)$$

In the case of phosphate ions (Fig. 4(c)), the IEP is not observed. Instead, the ζ potential is negative over the entire studied pH range, indicating a very strong adsorption of these ions on the surface [29]. Reports of NMR spectroscopy point

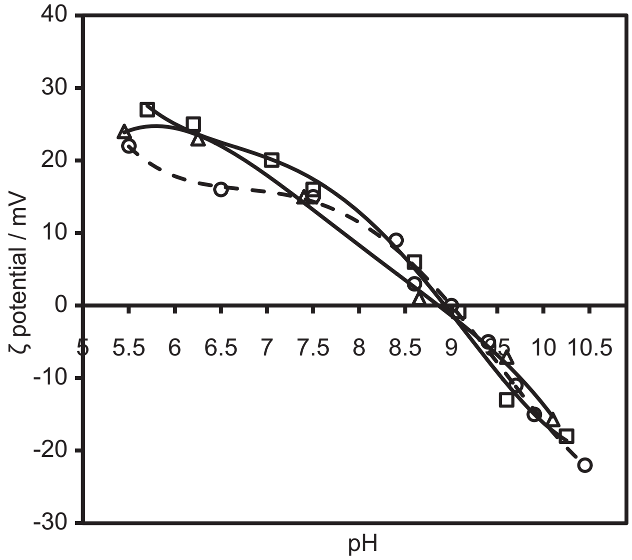

Fig. 3. ζ Potential as function of pH for NaCl solutions of 1 mM (squares), 10 mM (triangles) and 100 mM (circles).

out that the adsorption is through the formation of inner sphere complexes, such as monodentate (I) or bidentate (II, III) complexes [30,31].

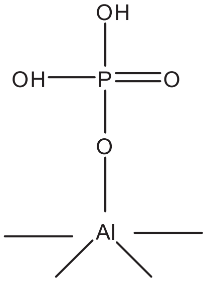

(I)

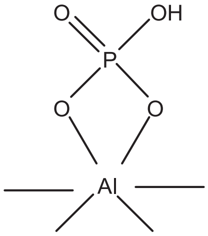

(II)

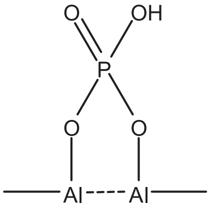

(III)

These are formed through a ligand exchange mechanism between a surface OH group bound to an aluminum atom and a phosphate ion, as can be seen in the following equation for the dihydrogen phosphate ion [32]:

$$\equiv \mathrm{AlOH} + \mathrm{H_2PO_4}^- \rightarrow \equiv \mathrm{AlOPO_3H_2} + \mathrm{OH}^- \tag{2}$$

Table 1 summarizes the results for calcium and phosphate adsorption with pH in the 7.4–8.6 range. Three differences are noted between calcium and phosphate uptake. First, phosphate adsorption is much higher than calcium adsorption. At pH 8.6 the adsorbed phosphate to adsorbed calcium ratio is almost 9, whereas at pH 7.4 this ratio increases to 96. Second, the higher the pH the higher the amount of calcium adsorbed. For phosphate, the opposite tendency is observed. In the case of calcium adsorption using pristine alumina, this tendency is very evident. At pH 8.6 this amount is approximately 8 times higher than the adsorbed at pH 7.4. However, regarding phosphate adsorption, it diminishes only around 25% in this pH range.

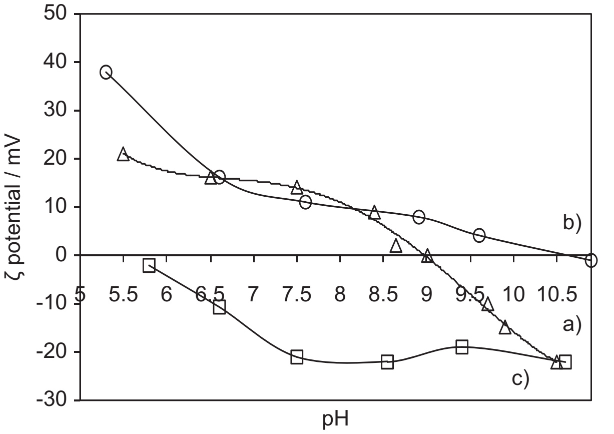

Fig. 4. ζ Potential as a function of pH in the presence of NaCl 100 mM (a), NaCl + $CaCl_2$ 1 mM (b) and NaCl = Na_2HPO_4 1 mM (c).

Finally, in the case of the alumina that has initially adsorbed phosphate ions, Al_2O_3–PO_4, calcium adsorption is higher than using the pristine alumina. This observation is more noticeable at pH 7.4. The former absorbs 10 times more calcium than the later. At pH 8 and 8.6 this increase is only 3 and 2 times, respectively. On the other hand, phosphate adsorption is only slightly higher when alumina that has previously uptaken calcium ions, Al_2O_3–Ca, is tested than if the pristine alumina is used. It varies from around 2% at pH 8.0 to almost 16% at pH 8.6. The higher tendency of alumina towards phosphate adsorption can be attributed to their opposite charges in the pH range studied.

Phosphate adsorbed onto a positive titanium oxide layer has been proposed as the first step for apatite nucleation [33]. Besides, it has been reported that phosphate groups present in organic monolayers formed on Ti and Au foils are effective apatite growth inducers [17,19]. However, in spite of the relative large amount of phosphate groups that were adsorbed on the positive alumina surface at pH 7.4 (around 0.5 group/nm^2), it did not show apatite-forming ability using a calcium-phosphate solution at this pH. In this case we observed a higher consumption of phosphate than calcium ions in each one of the alumina immersions in the calcium-phosphate solution. The total phosphate to calcium uptake ratio after 16 days was around 4.5, but

Table 1
Calcium and phosphate adsorption on the pristine alumina (Al_2O_3) and on alumina that has previously adsorbed phosphate (Al_2O_3–PO_4) and calcium (Al_2O_3–Ca).

pH	Calcium adsorption × 10^5 (mol/g)		Phosphate adsorption × 10^5 (mol/g)		Ca adsorption on sorbed PO_4 × 10^5 (mol/g)fna;[a]	PO_4–Ca/Al_2O_3–PO_4
	Al_2O_3 (a)	Al_2O_3–PO_4 (b)	Al_2O_3 (c)	Al_2O_3–Ca	(b) − (a) = (d)	(d)/(c)
7.4	0.275	2.69	26.5	29.7	2.41	0.09
8.0	1.39	4.25	25.8	26.2	2.86	0.11
8.6	2.24	5.31	19.7	22.6	3.07	0.16

[a] Calculated assuming that the difference on Ca adsorption is totally due to the phosphate first attached to alumina.

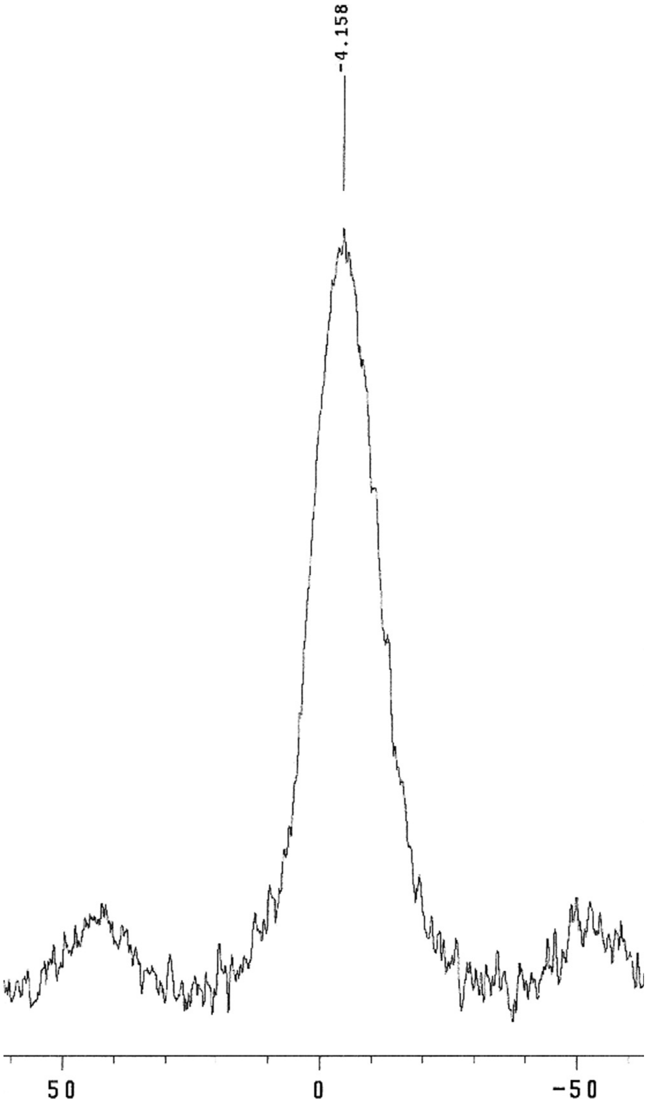

Fig. 5. ^{31}P MAS-NMR spectrum of the alumina immersed initially in a Na_2HPO_4 solution at pH 7.4, then in a $CaCl_2$ solution and in the calcium-phosphate solution at pH 7.4 for 2 weeks at room temperature.

apatite or other calcium phosphate could not be detected by means of TEM, Raman spectroscopy or NMR. The ^{31}P MAS-NMR analysis showed only one peak at −4.158 ppm (Fig. 5), which is similar to the reported [30] for phosphate adsorbed on alumina, but does not correspond to any calcium phosphate.

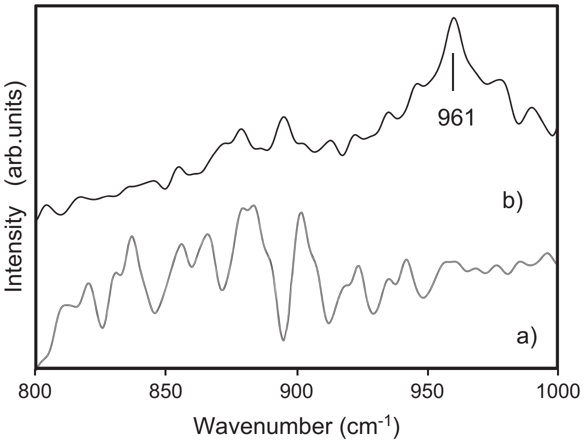

Fig. 6. Raman spectra of the alumina immersed initially in a Ca solution at pH 11.3, and then in a Na_2HPO_4 solution at pH 8.6 (a) and of the alumina immersed initially in the Ca solution at pH 11.3, then in a Na_2HPO_4 solution at pH 8.6 and finally in the calcium-phosphate solution at pH 8.6 and 30 °C, for 3 h lapses (b).

On the contrary, apatite growth was observed if the alumina initially immersed at pH 11.3 on a calcium solution, Al_2O_3–Ca, was later immersed on a phosphate solution at pH 8.6 and finally resuspended several times in the calcium-phosphate solution at pH 8.6. Fig. 6 shows the Raman spectra of the alumina immersed in the alumina thus treated before (Fig. 6(a)) and after the immersion in the calcium-phosphate solution at pH 8.6 (Fig. 6(b)). The band at 961 cm^{-1}, which is absent on the spectrum of the substrate that only adsorbed once phosphate ions (Fig. 6(a)), is close to the ν_1 phosphate vibrational mode for calcium hydroxyapatites, 962 cm^{-1} [34]. Fig. 7 corresponds to the ^{31}P MAS-NMR spectrum of the alumina immersed in the calcium-phosphate solution at pH 8.6. It can be seen only a single peak at 2.817 ppm, which is within the ^{31}P chemical shifts reported for hydroxyapatites, 2.8 ± 0.2 ppm [35]. Fig. 8(a) and (b) shows a bright field TEM image and a selected area electron diffraction pattern of the solid obtained at pH 8.6, respectively. Clear differences can be seen with Fig. 2. While for the alumina substrate the electron diffraction pattern shows a strong amorphous halo corresponding to the amorphous alumina, the showed rings in Fig. 8(b) correspond to the (211), (222), and (511) planes of hydroxyapatite, $Ca_5(PO_4)_3OH$ (JCPDF 24-0033). Besides, it can be seen that apatite grew as tiny crystals (Fig. 8(a)) on the alumina substrate (Fig. 2(a)).

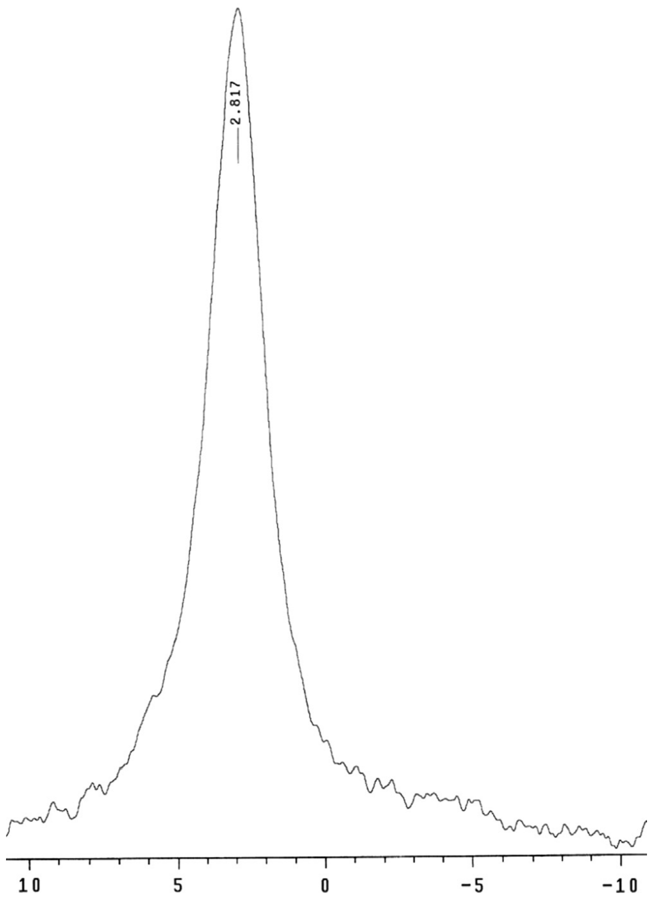

Fig. 7. ^{31}P MAS-NMR spectrum of the alumina immersed initially in a Ca solution at pH 11.3, then in a Na_2HPO_4 solution at pH 8.6 and finally in the calcium-phosphate solution at pH 8.6 and 30 °C, for 3 h lapses.

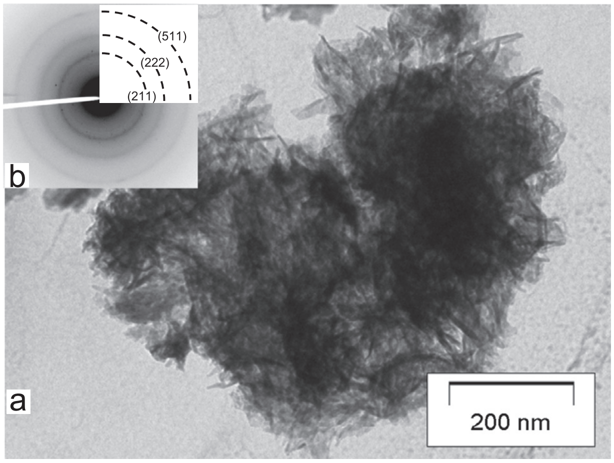

Fig. 8. TEM photograph (a) and selected area electron diffraction pattern (b) of the alumina immersed initially in a Ca solution at pH 11.3, then in a Na_2HPO_4 solution at pH 8.6 and finally in the calcium-phosphate solution at pH 8.6 and 30 °C, for 3 h lapses.

According to the previous results, the different abilities towards apatite formation on the studied alumina seem to be related to the initial adsorption of calcium or phosphate ions.

Apatite growth at pH 8.6 may be attributed to the high proportion of $\equiv AlOCa^+$ sites formed during the first immersion on a Ca solution at pH 11.3 (around 0.25 sites/nm^2), and to the fact that the capacity of adsorption of the Al_2O_3–Ca substrate towards phosphate ions is stronger than that of the Al_2O_3–PO_4 sites towards Ca ions. Although we observed a noticeable increase on Ca adsorption using the Al_2O_3–PO_4 substrate, only a small fraction of the total adsorbed phosphate sites at pH 7.4 are able to uptake Ca ions, around 9%, whereas the amount of phosphate adsorbed on the Al_2O_3–Ca substrate is close to the number of Al_2O_3–Ca sites at pH 8.6: 2.9 and 2.24 mol/g, respectively (Table 1).

Inertness of alumina towards apatite formation has been attributed to is positive surface charge at pH 7.4. It has been reported that a negative surface charge is necessary for apatite growth because it attracts calcium ions, which seems to be the first step on apatite heterogeneous nucleation [1,3,9,23]. However, during apatite growth on $CaTiO_3$, which shows a positive surface at pH 7.4, phosphate consumption precedes calcium uptake [14,36]. Similarly, it was reported that a positive titanium oxide layer showed a high apatite-forming ability [33]. Thus, it seems that the positive surface charge of alumina could not have a determining role influencing its *in vitro* inertness towards apatite growth at pH 7.4, as has been proposed. Apparently, this could be attributed to a low attraction of the phosphate complexes initially formed towards a subsequent calcium adsorption (Table 1), or to the formation of stable surface clusters, such as (IV), showing no reactivity for apatite nucleation.

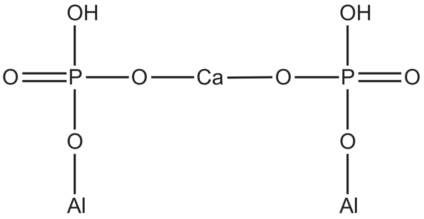

(IV)

On the other hand, although the initial Ca adsorption at pH 11. 3 seems to favor the apatite nucleation, it is possible that the scarce number of Al_2O_3–Ca sites formed at pH 7.4, around 5×10^{-3} sites/nm^2, could also explain the lack of alumina bioactivity *in vitro* at this pH.

Results shown in the present work could help to better understand the heterogeneous apatite nucleation of alumina *in vitro*, thus leading to the design of more effective bioactive materials.

4. Conclusions

The studied alumina bears a positive surface charge at pH 7.4 and has a strong tendency for phosphate adsorption, but it shows only a slight attraction towards calcium ions at this pH. Phosphate adsorption turns the surface negative and increases calcium uptake, but apatite formation could not be detected when alumina with adsorbed phosphate and calcium ions was immersed in a calcium-phosphate solution at pH 7.4. However, apatite growth was observed at pH 8.6 using alumina initially immersed on a Ca solution at pH 11.3. This treatment increases calcium adsorption noticeably compared with the uptake at pH 7.4. The formed AlOCa$^+$ sites increase the further phosphate uptake, and favors apatite nucleation. The lack of *in vitro* bioactivity of alumina at pH 7.4 does not seem to be related to its positive surface charge, but to the formation of stable surface alumina-phosphate complexes showing a very low tendency towards calcium adsorption.

Acknowledgments

Authors would like to thank Q. Aurora Mendez Marzo for her kind help in the performance of the zeta potential experiments in the present and our previous work. Also we acknowledge Ing. Patricia Castillo for the TEM images, Dra. Yolanda Marmolejo for the Raman spectra and Dr Guillermo Mendoza for the NMR spectra.

References

[1] T. Kokubo, H.M. Kim, M. Kawashita, Novel bioactive materials with different mechanical properties, Biomaterials 24 (2003) 2161–2175.

[2] M. Tanahashi, T. Yao, T. Kokubo, M. Minoda, T. Miyamoto, T. Nakamura, T. Yamamuro, Apatite coated on organic polymers by biomimetic process: improvement in its adhesion to substrate by glow-discharge treatment, J. Biomed. Mater. Res. A 29 (1995) 349–357.

[3] M.M. Pereira, L.L. Hench, Mechanism of hydroxyapatite formation on porous gel-silica substrates, J. Sol–Gel Sci. Technol. 7 (1996) 59–68.

[4] P. Li, C. Ohtsuki, T. Kokubo, K. Nakanishi, N. Soga, T. Nakamura, T. Yamamuro, Apatite formation induced by silica gel in a simulated body fluid, J. Am. Ceram. Soc. 75 (1992) 2094–2097.

[5] O.H. Andersson, K.H. Karlsson, On the bioactivity of silicate glass, J. Non-Cryst. Solids 129 (1991) 145–151.

[6] X. Liao, H. Zhu, G. Yin, Z. Huang, Y. Yao, X. Chen, *In vitro* bioactivity and cytocompatibility of tricalcium silicate, Bull. Mater. Sci. 34 (2011) 1151–1155.

[7] S.B. Cho, K. Nakanishi, T. Kokubo, N. Soga, C. Ohtsuki, T. Nakamura, Apatite formation on silica gel in simulated body fluid: its dependence on structures of silica gels prepared in different media, J. Biomed. Mater. Res. B: Appl. Biomater. 33 (1996) 145–151.

[8] J. Liu, X. Miao, Sol–gel derived bioglass as a coating material for porous alumina scaffolds, Ceram. Int. 30 (2004) 1781–1785.

[9] R. Viitala, M. Jokinen, T. Peltola, K. Gunnelius, J.B. Rosenholm, Surface properties on *in vitro* bioactive and non-bioactive sol–gel derived materials, Biomaterials 23 (2002) 3073–3086.

[10] M. Jokinen, M. Pätsi, H. Rahiala, T. Peltola, M. Ritala, J.B. Rosenholm, Influence of sol and surface properties on *in vitro* bioactivity of sol–gel-derived TiO_2–SiO_2 films deposited by dip-coating method, J. Biomed. Mater. Res. 42 (1998) 295–302.

[11] T. Peltola, M. Jokinen, H. Rahiala, M. Pätsi, J. Heikkilä, I. Kangasniemi, A. Yli-Urpo, Effect of aging time of sol on structure and *in vitro* calcium phosphate formation of sol–gel derived titania films, J. Biomed. Mater. Res. 51 (2000) 200–208.

[12] P. Li, I. Kangasniemi, K. de Groot, T. Kokubo, Bonelike hidroxyapatite induction by a gel-derived titania on a titanium substrate, J. Am. Ceram. Soc. 77 (1994) 1307–1312.

[13] B.C. Yang, J. Weng, X.D. Li, X.D. Zhang, The order of calcium and phosphate ion deposition on chemically treated tiatanium surfaces soaked in aqueous solution, J. Biomed. Mater. Res. 47 (1999) 213–219.

[14] J. Coreño, O. Coreño, Evaluation of calcium titanate as apatite growth promoter, J. Biomed. Mater. Res. A 75 (2005) 478–484.

[15] T. Miyazaki, H.M. Kim, F. Miyaji, T. Kokubo, H. Kato, T. Nakamura, Bioactive tantalum metal prepared by NaOH treatment, J. Biomed. Mater. Res. 50 (2000) 35–42.

[16] M. Uchida, H.M. Kim, T. Kokubo, F. Miyaji, T. Nakamura, Bonelike apatite formation induced on zirconia gel in a simulated body fluid and its modified solutions, J. Am. Ceram. Soc. 84 (2001) 2041–2044.

[17] M. Tanahashi, T. Matsuda, Surface functional group dependence on apatite formation on self-assembled monolayers in a simulated body fluid, J. Biomed. Mater. Res. 34 (1997) 305–315.

[18] K. Sato, Y. Kumagai, J. Tanaka, Apatite formation on organic monolayers in simulated body environment, J. Biomed. Mater. Res. A 50 (2000) 16–20.

[19] Q. Liu, J. Ding, F.K. Mante, S.L. Wunder, G.R. Baran, The role of surface functional groups in calcium phosphate nucleation on titanium foil: a self-assembled monolayer technique, Biomaterials 23 (2002) 3103–3111.

[20] C.R. Rambo, F.A. Müller, L. Müller, H. Sieber, I. Hofmann, P. Greil, Biomimetic apatite coating on biomorphous alumina scaffolds, Mater. Sci. Eng. C: Mater. Biol. Appl. 26 (2006) 92–99.

[21] F. Barrère, A. Lebugle, C.A. van Blitterwijk, K. de Groot, P. Layrolle, C. Rey, Calcium phosphate interaction with titanium oxide and alumina substrates: an XPS study, J. Mater. Sci. Mater. Med. 14 (2003) 419–425.

[22] P. Li, C. Ohtsuki, T. Kokubo, K. Nakanishi, N. Soga, K. de Groot, The role of hydrated silica, titania and alumina in inducing apatite on implants, J. Biomed. Mater. Res. A 28 (1994) 7–15.

[23] M. Kawashita, A. Kamitani, T. Miyazaki, N. Matsui, A. Li, H. Kanetaka, M. Hashimoto, Mater. Sci. Eng. C: Mater. Biol. Appl. 32 (2012) 2617–2622.

[24] H.H. Lu, S.R. Pollack, P. Ducheyne, Temporal zeta potential variations of 45S5 bioactive glass immersed in an electrolyte solution, J. Biomed. Mater. Res. 51 (2000) 80–87.

[25] M.H. Juárez, R.J.M. Martínez, L.J.M. Rubalcava, P.O. Vargas, R.J. Serrato, Aluminum oxide and hydroxides from non-bauxitic sources, Am. Ceram. Soc. Bull. 76 (1997) 55–59.

[26] J.S. Reed, Principles of Ceramics Processing, second ed., John Wiley-Interscience, New York, 1995.

[27] C.P. Huang, W. Stumm, Specific adsorption of cations on hydrous γ-alumina, J. Colloid Interface Sci. 43 (1973) 409–420.

[28] W.B. Samuel de Lint, N.E. Benes, J. Lyklema, H.J.M. Bouwmeester, A.J. van der Linde, M. Wessling, Ion adsorption parameters determined from zeta potential and titration data for a γ-alumina nanofiltration membrane, Langmuir 19 (2003) 5861–5868.

[29] R.J. Hunter, in: Zeta Potential in Colloid Science: Principles and Applications, second ed., Academic Press, London, 1988.

[30] Y. Kim, R.J. Kirkpatrick, An investigation of phosphate adsorbed on aluminum oxyhydroxide and oxide phases by nuclear magnetic resonance, Eur. J. Soil Sci. 55 (2004) 243–251.

[31] R. Lookman, P. Grobet, R. Merckx, K. Vlassak, Phosphate sorption by synthetic amorphous aluminum hydroxides: a ^{27}Al and ^{31}P solid-state MAS NMR spectroscopy study, Eur. J. Soil Sci. 45 (1994) 37–44.

[32] S. Goldberg, G. Sposito, On the mechanism of specific phosphate adsorption by hydroxylated mineral surfaces: a review, Commun. Soil Sci. Plant Anal. 16 (1985) 801–821.

[33] D.K. Pattanayak, S. Yamaguchi, T. Matsushita, T. Kokubo, Effect of heat treatments on apatite-forming ability of NaOH- and HCl- treated titanium metal, J. Mater. Sci. Mater. Med. 22 (2011) 273–278.

[34] P.N. de Aza, F. Guitián, C. Santos, S. de Aza, R. Cuscó, L. Artús, Vibrational properties of calcium phosphates compounds. 2. Comparison between hydroxyapatite and β tricalcium phosphate, Chem. Mater. 9 (1997) 916–922.

[35] W.P. Rothwell, J.S. Waugh, J.P. Yesinowski, High-resolution variable temperature ^{31}P NMR of solid calcium phosphates, J. Am. Chem. Soc. 102 (1980) 2637–2643.

[36] T. Hanawa, M. Kon, H. Doi, H. Ukai, K. Murakami, H. Hamanaka, K. Asaoka, Amount of hydroxyl radical on calcium-ion-implanted titanium and point of zero charge of constituent oxide of the surface-modified layer, J. Mater. Sci. Mater. Med. 9 (1998) 89–92.